Coordination in the Gas Phase

DOI: 10.1002/ange.200604148

The Search for the Species with the Highest Coordination Number**

*Andreas Hermann, Matthias Lein, and Peter Schwerdtfeger**

The question of the highest possible coordination number for an atom is addressed as this is related to the Gregory–Newton problem of kissing hard spheres.[1] Using first-principles quantum chemical simulations we show that the interaction of Pb^{2+} with He atoms results in remarkably stable $PbHe_{15}^{2+}$ with 15 atoms in the first coordination sphere forming a Frank–Kasper polyhedron.[2] The Pb–He distances do not change significantly by subsequent filling of the first coordination shell as one expects for a hard-sphere model. Such high coordination numbers have been proposed only in liquid simulations so far.[3]

The problem of how many spheres (N_{max}, called the kissing number or Newton number) of a given radius R can be packed around a unit sphere in n_{dim} dimensions is called the generalized Gregory–Newton problem. In three dimensions, if all spheres have the same radius, the answer is well known: $N_{max} = 12$.[1] The extension to general dimensions (with the exception of $n_{dim} = 1$, 2, 3, 8, and 24), or the kissing-number problem of spheres with radius R on a unit sphere, remains unsolved.[1]

In chemistry N_{max} corresponds to the maximum coordination number of ligands interacting with a central atom, as pointed out as early as 1875 by Günther.[4] Herein we assume that the ligands do not interact strongly with each other. Hence this excludes systems like $M@C_{60}$, which would have $N_{max} = 60$ but are better described as an atom trapped in a fullerene cage.

It is well known that regular icosahedral structures with $N = 12$ in the first coordination sphere are particularly stable and are found, for example, in rare-gas clusters and in a number of metallic clusters.[5] Such high coordination numbers are also found in actinide complexes, for example in $[U(NO_3)_6]^{2-}$ [6] and $[Th(NO_3)_6]^{2-}$.[7] In the solid state, coordination numbers up to $N_{max} = 12$ (hexagonal closed packing and face-centered cubic) are realized, and high coordination numbers usually imply denser packing. In liquid-metal simulations, coordination numbers as high as 16 or higher have been postulated but only for a very short timeframe.[3,8] In binary intermetallic alloys local coordination numbers of 14, 15, and even 16 are predicted; prime examples are Friauf–Laves phases in $MgZn_2$ or $MgNi_2$.[9] Frank and Kasper showed that the frequent use of icosahedral coordination will occur in conjunction with coordination numbers higher than 12 stabilized by the surrounding matrix.[2]

Herein we take a different approach. We look for a single molecule MX_N in the gas phase of high coordination number N which can be experimentally verified. We choose a large positively charged central atom, $M = Pb^{2+}$, and a very small ligand, X = He. Both atoms have reasonably small polarizabilities ($\alpha_{He} = 1.38$ au[10] and $\alpha_{Pb^{2+}} = 14.1$ au[11]), and therefore fit the hard-sphere model quite well. The ionization potential of Pb^+ (15.03 eV) is much smaller than that of He (24.58 eV).[12] Hence, Pb^{2+}–He does not undergo a Coulomb explosion and there is no (or minimal) charge transfer from He to Pb^{2+}. Hence the Pb^{2+}–He interaction $V(R)$ is mainly of charge-induced-dipole (CID) nature [Eq. (1) with the charge $q_{Pb} = +2e$]. There is also little interaction (mainly of van der Waals type) between the helium atoms on the coordination sphere. We employed both wavefunction as well as density-functional-based methods in our calculations to calculate the Pb^{2+}–He potential energy curves shown in Figure 1.

$$V_{CID}(R) = -q_{Pb}^2 \alpha_{He}/2R^4 \quad (1)$$

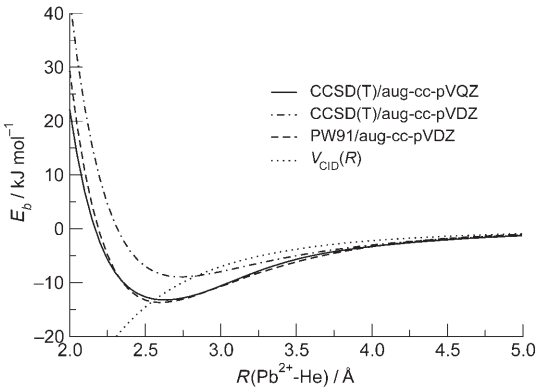

Figure 1. Potential energy curves for $PbHe^{2+}$ using various theoretical methods. The CID curve is also shown. Binding energies E_b and bond lengths R_e: CCSD(T)/aug-cc-pVQZ 13.22 kJ mol^{-1} and 2.629 Å; CCSD(T)/aug-cc-pVDZ 8.97 kJ mol^{-1} and 2.738 Å; PW91/aug-cc-pVDZ 13.70 kJ mol^{-1} and 2.595 Å.

In Figure 2 the optimized structures for $PbHe_N^{2+}$ with $N \leq 12$ are shown as obtained from density functional calculations. Additionally, in Table 1 the average Pb–He and He–He distances on the coordination sphere are given. The average Pb–He distance increases monotonically with increasing N, whereas the average He–He distance in the outer shell decreases (not monotonically) as one expects. The "small-N" structures up to $N = 7$ deviate strongly from an equally spaced He distribution around the central Pb. Instead,

[*] A. Hermann, Dr. M. Lein, Prof. Dr. P. Schwerdtfeger
Center of Theoretical Chemistry and Physics
Institute of Fundamental Sciences
Massey University (Auckland Campus)
Private Bag 102904, North Shore MSC, Auckland (New Zealand)
Fax: (+64) 9-373-422
E-mail: p.a.schwerdtfeger@massey.ac.nz

[**] This work was financed by a Marsden grant through the Royal Society of New Zealand.

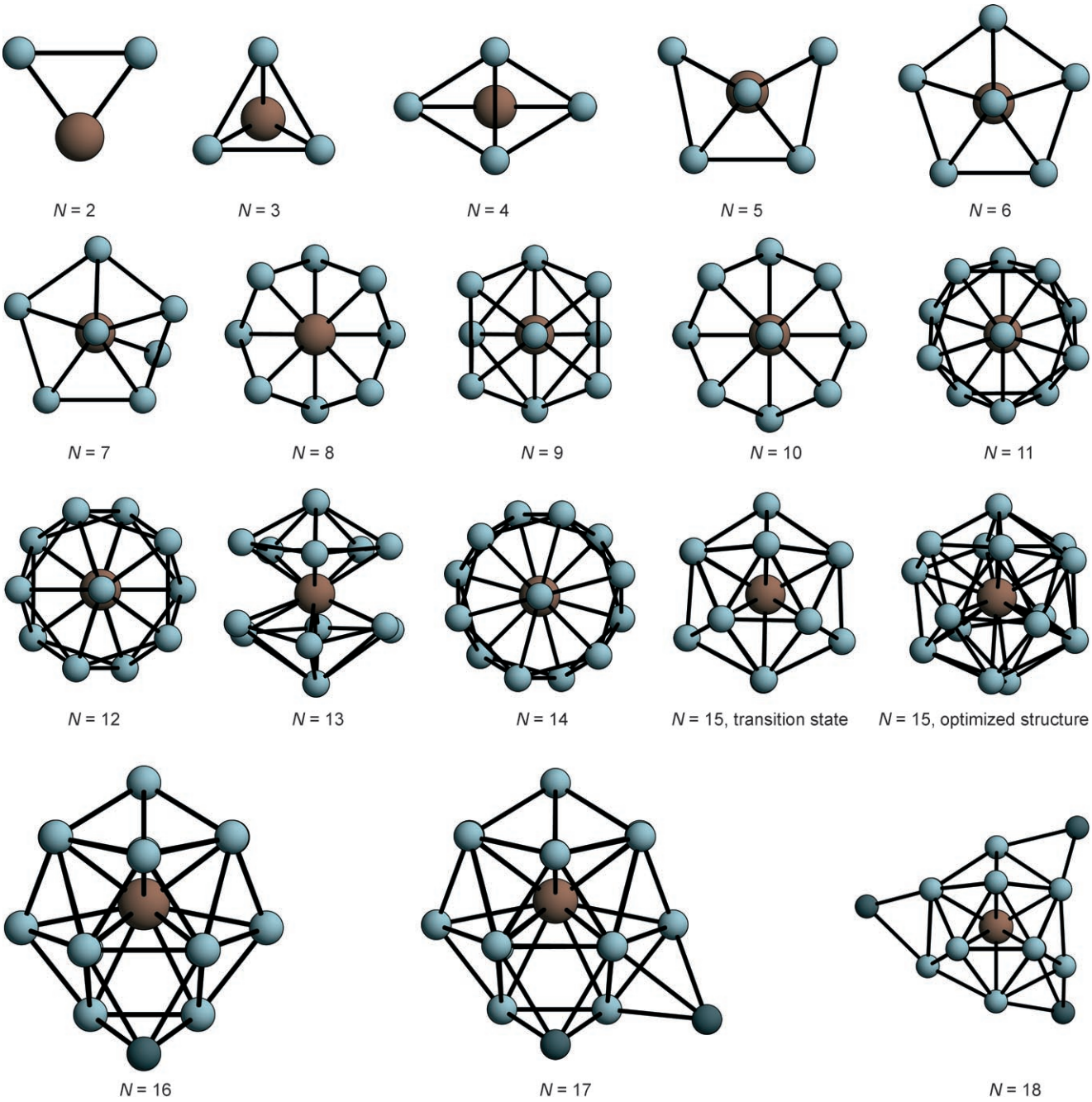

Figure 2. Optimized $PbHe_N^{2+}$ structures for $N \leq 18$. For $N > 15$ the dark-gray He atoms denote atoms of the second shell.

up to $N = 6$, all He atoms lie in the same half sphere, arranged into a part of an icosahedral distribution (Figure 2). This is due to small van der Waals interactions between the He atoms. For $N = 6$, for example, the structure with equally distributed He atoms (which is not a local minimum) is only 0.51 kJ mol^{-1} above the global minimum structure. We also observe almost no charge transfer from He to Pb^{2+}; the Coulomb repulsion of the weakly charged He atoms is therefore small ($q_{He} = +0.012\,e$ for $N = 6$).

From $N = 8$ onwards, the structures resemble closely He atoms equally distributed around the Pb atom. More interesting are the structures with $N \geq 12$ as we find structural minima for N up to 15. Thus, we report for the first time a stable gas-phase structure with a coordination number higher than 12.

For $N = 12$ the optimized icosahedral structure equals the corresponding Frank–Kasper polyhedron (FKP). For $N = 13$, no such polyhedron exists. Instead, the optimized structure contains an "upper" half that equals half of the $N = 12$ FKP, and a "bottom" half that equals half of the $N = 14$ FKP. For $N = 14$ we get again the FKP as optimized structure. In the $N = 15$ case, the ideal FKP is a transition state (first-order saddle point) and the minimum is a distorted FKP (see Figure 2). We interpret this as a sign that the limit of structural stability is reached. Indeed, if we increase N to 16 or higher, we do not find a minimum structure where all He atoms are

Table 1: Minimum, maximum, and average Pb–He distances, and average He–He distances for $PbHe_N^{2+}$ (in Å). For the He–He average distance only the atoms in close contact with $R \leq 3.1$ Å are chosen.

N	R_{min}(Pb–He)	R_{max}(Pb–He)	R_{av}(Pb–He)	R_{av}(He–He)
1	2.595	2.595	2.595	
2	2.602	2.602	2.602	3.054
3	2.606	2.608	2.607	3.096
4	2.612	2.629	2.621	3.079
5	2.619	2.642	2.634	3.062
6	2.621	2.652	2.646	3.001
7	2.634	2.676	2.660	3.019
8	2.668	2.672	2.670	3.244
9	2.679	2.683	2.681	3.098
10	2.689	2.697	2.694	2.924
11	2.702	2.721	2.712	2.877
12	2.720	2.722	2.722	2.862
13	2.716	2.802	2.759	2.776
14	2.712	2.802	2.789	2.739
15	2.754	2.869	2.825	2.662

positioned in the first shell around the Pb atom. Hence for $PbHe_N^{2+}$ we get $N_{max} = 15$. This is larger than in the previously studied YHe_N^{3+} system where only an icosahedral coordination has been achieved as the maximum, $N_{max} = 12$.[13] Figure 3

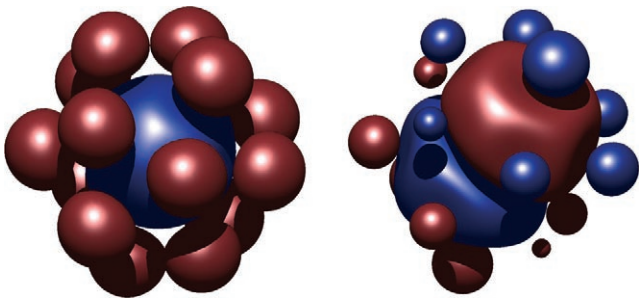

Figure 3. Isosurface plots of the HOMO (left) und LUMO (right) of $PbHe_{15}^{2+}$. Isosurface value $\rho = 0.01$ au.

shows isosurface plots of the highest occupied (HOMO) und lowest unoccupied (LUMO) states of the $PbHe_{15}^{2+}$ molecule. The HOMO mainly consists of slightly polarized He 1s orbitals antibonding to the Pb 6s orbital. The LUMO is mainly of Pb 6p character, as expected. The plots illustrate that the bonding of He to Pb is of CID nature.

The incremental binding energy (E_{IB}) for each molecule as shown in Figure 4 is given by Equation (2), where $E_b(N)$ is the binding energy of $PbHe_N^{2+}$ and $E(He)$ is the total energy of He. $E_{IB}(N)$ is the energy gain upon attaching an additional He atom to a $PbHe_{N-1}^{2+}$ molecule. For $N < 12$ E_{IB} decreases (in absolute values) with increasing N. However, there is a local maximum at $N = 12$, indicating the especially stable icosahedral structure. As expected, E_{IB} is much smaller for $N = 13$, an indication of the rather unstable configuration seen in Figure 2. For the first time, a second local maximum at $N = 14$ was shown, where again the very stable FKP structure is adopted. For $N = 15$, E_{IB} decreases again, a signal that the structural-stability limit is reached. For $N = 16$, the energy of the transition-state one-shell structure is given, that shows a

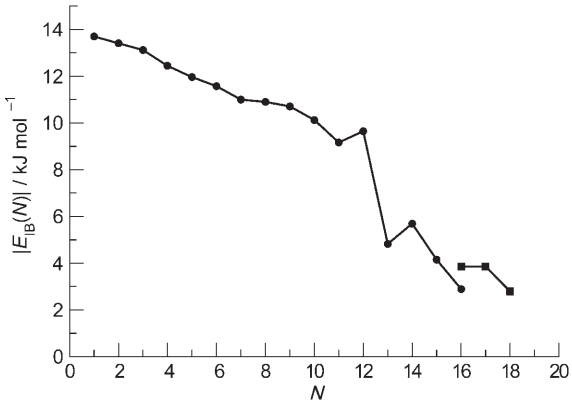

Figure 4. E_{IB} for $PbHe_N^{2+}$. Circles: minima of one-shell structures; squares: minima of two-shell structures.

further decrease of E_{IB}. From that point on, two-shell structures are more favored (squares in Figure 4 for $N = 16$–18). In these structures, one or more He atoms are in a second geometrical shell, whereas the inner shell consists of 15 He atoms (see Figure 2). Interestingly, we were not able to construct two-shell systems, where the inner shell consists of 14 He atoms or less. In such cases, He atoms from the outer shell always diffused into the inner shell during the optimization procedure to form a first coordination shell of 15 atoms. This further supports our opinion that the $PbHe_{15}^{2+}$ molecule is a stable one-shell system. The stability of $PbHe_{15}^{2+}$ suggests that it can be identified by mass spectrometric methods.

$$E_{IB}(N) = E_b(N) - E_b(N-1) - E(He) \quad (2)$$

Methods

Of all the density functionals (DFT) tested for $PbHe^{2+}$ the gradient-corrected Perdew–Wang functional (PW91)[14] performed better than extensive coupled-cluster calculations[15] using an aug-cc-pVQZ basis set for both He[17] and Pb.[18] In fact, for the PW91 calculations, the potential curve is already well described with the smaller aug-cc-PVDZ basis sets, which are therefore used for the cluster calculations.[16] Where computationally feasible (for the smallest clusters) we optimized the structures at the CCSD(T)-level of theory using the large aug-cc-PVQZ basis sets and these results are in good agreement with the PW91 results (see Figure 1). Rather extensive second-order perturbation theory calculations for electron correlation (MP2) and hybrid-DFT (B3LYP) calculations[16] for $PbHe_{15}^{2+}$ with double-zeta-quality basis sets both verified that the global minimum is the one with 15 He atoms in the first coordination shell. The Pb atom was approximated by an energy-consistent scalar relativistic pseudopotential including 20 electrons in the valence space.[19]

For all structures, the starting point in the search for the global minimum was an equal spatial distribution of the He atoms on a sphere of reasonable radius around the central Pb atom. The respective distributions were determined numerically by damped relaxation of a set of Coulomb-repulsing particles on the unit sphere. The Hessian for the atom displacements was checked to assure that minimum structures are obtained. Different distributions lead to the location of the global minimum structure. We have also searched for other positively charged ions interacting with He which are easily accessible to future experiments, for example Cs^+ or Ba^{2+}. However,

Pb^{2+} gave the most stable clusters with the highest coordination number. We note that higher coordination number might be expected for charged actinide–He interactions, for example, UHe_N^{q+} ($q = 1$–3), but these are more difficult to study by theoretical and experimental methods.

Received: October 10, 2006
Published online: February 21, 2007

Keywords: coordination modes · density functional calculations · dipole interactions · Gregory–Newton problem · lead

[1] N. J. A. Sloane, J. H. Conway, *Sphere Packings, Lattices and Groups*, Springer, New York, **1999**.
[2] F. C. Frank, J. S. Kasper, *Acta Crystallogr.* **1958**, *11*, 184 – 190.
[3] C. Bichara, A. Pellegatti, J.-P. Gaspard, *Phys. Rev. B* **1993**, *47*, 5002 – 5007.
[4] S. Günther, *Arch. Math. Phys.* **1875**, *57*, 209 – 215.
[5] R. L. Johnston, *Atomic and Molecular Clusters*, Francis, London, **2002**.
[6] J. Rebizant, C. Apostolidis, M. R. Spirlet, G. D. Andreeti, B. Kanellakopulos, *Acta Crystallogr. Sect. C* **1988**, *44*, 2098 – 2101.
[7] U. Abram, E. Bonfada, E. Schulz Lang, *Acta Crystallogr. Sect. C* **1999**, *55*, 1479 – 1482.
[8] H. W. Sheng, W. K. Luo, F. M. Alamgir, J. M. Bai, E. Ma, *Nature* **2006**, *439*, 419 – 425.
[9] Y. Komura, K. Tokunaga, *Acta Crystallogr. Sect. B* **1980**, *36*, 1548 – 1554.
[10] A. C. Newell, R. C. Baird, *J. Appl. Phys.* **1965**, *36*, 3751 – 3759.
[11] Calculated using the pseudopotential and accompanying aug-cc-pVQZ basis set as described in the Methods Section. The small polarizability of Pb^{2+} is due to the relativistic 6s contraction.
[12] C. E. Moore, *Atomic Energy Levels*, US GPO, Washington, **1958**.
[13] R. Wesendrup, G. E. Moyano, M. Pernpointner, P. Schwerdtfeger, *J. Chem. Phys.* **2002**, *117*, 7506 – 7511.
[14] J. P. Perdew, K. Burke, Y. Wang, *Phys. Rev. B* **1996**, *54*, 16533 – 16539.
[15] R. J. Bartlett, *J. Phys. Chem.* **1989**, *93*, 1697 – 1708.
[16] Gaussian 03, Revision C.02, M. J. Frisch, G. W. Trucks, H. B. Schlegel, G. E. Scuseria, M. A. Robb, J. R. Cheeseman, J. A. Montgomery, Jr., T. Vreven, K. N. Kudin, J. C. Burant, J. M. Millam, S. S. Iyengar, J. Tomasi, V. Barone, B. Mennucci, M. Cossi, G. Scalmani, N. Rega, G. A. Petersson, H. Nakatsuji, M. Hada, M. Ehara, K. Toyota, R. Fukuda, J. Hasegawa, M. Ishida, T. Nakajima, Y. Honda, O. Kitao, H. Nakai, M. Klene, X. Li, J. E. Knox, H. P. Hratchian, J. B. Cross, V. Bakken, C. Adamo, J. Jaramillo, R. Gomperts, R. E. Stratmann, O. Yazyev, A. J. Austin, R. Cammi, C. Pomelli, J. W. Ochterski, P. Y. Ayala, K. Morokuma, G. A. Voth, P. Salvador, J. J. Dannenberg, V. G. Zakrzewski, S. Dapprich, A. D. Daniels, M. C. Strain, O. Farkas, D. K. Malick, A. D. Rabuck, K. Raghavachari, J. B. Foresman, J. V. Ortiz, Q. Cui, A. G. Baboul, S. Clifford, J. Cioslowski, B. B. Stefanov, G. Liu, A. Liashenko, P. Piskorz, I. Komaromi, R. L. Martin, D. J. Fox, T. Keith, M. A. Al-Laham, C. Y. Peng, A. Nanayakkara, M. Challacombe, P. M. W. Gill, B. Johnson, W. Chen, M. W. Wong, C. Gonzalez, J. A. Pople, Program Gaussian, Inc., Wallingford, CT, **2004**.
[17] D. E. Woon, T. H. Dunning, Jr., *J. Chem. Phys.* **1994**, *100*, 2975 – 2988.
[18] K. A. Peterson, *J. Chem. Phys.* **2003**, *119*, 11099 – 11112.
[19] B. Metz, H. Stoll, M. Dolg, *J. Chem. Phys.* **2000**, *113*, 2563 – 2569; the Stuttgart pseudopotentials and corresponding valence basis sets can be obtained from the website http://www.theochem.uni-stuttgart.de.

